

Improved flow rate and pressure ANN estimators for a centrifugal fan with an induction motor drive

Cebraıl Turkeri * 

University of Warwick, School of Engineering, CV47AL, Coventry, UK, cebrail.turkeri@warwick.ac.uk

Oleh Kiselychnyk 

University of Warwick, School of Engineering, CV47AL, Coventry, UK, o.kiselychnyk@warwick.ac.uk

Submitted: 21.02.2023
Accepted: 24.08.2024
Published: 30.09.2024



* Corresponding Author

Abstract: Energy saving control algorithms of centrifugal fans/pumps are based on the use of the frequency-controlled induction motor drives and pressure or flow rate sensors, the costs of which are comparable to the cost of the fans/pumps for low-power applications. The paper develops a new and simple estimation approach of the pressure and flow rate, utilising the measured Root Mean Square (RMS) value of the stator current, estimated motor's input active power, reference stator voltage frequency and feed-forward backpropagation artificial neural network. The error percentage for both flow rate and pressure in experimental and estimated data is within the range of $\pm 5\%$, which conforms to the ISO 13348 standard. A test rig for the rapid control prototyping of the fan is designed, and necessary design and test procedures are developed. The estimation approach is verified experimentally and demonstrates better estimation accuracy compared to the existing and possible similar simple approaches. The developed algorithm can be easily embedded into the industrial variable frequency drives without any hardware changes.

Keywords: *Artificial Neural Network, Centrifugal Fan, Industrial Power Systems, Sensorless Industrial Application*

Cite this paper as: Turkeri, C., & Kiselychnyk, O. Improved flow rate and pressure ANN estimators for a centrifugal fan with an induction motor drive. *Journal of Energy Systems* 2024; 8(3): 130-142, DOI: 10.30521/jes.1254552

2024 Published by peer-reviewed open access scientific journal, JES at DergiPark (<https://dergipark.org.tr/jes>)

1. INTRODUCTION

Water and air supplies are essential in many industrial applications. In Europe, pumps and fans that deliver these resources consume through their electrical drives approximately 22% and 16% of the total electricity demand, respectively [1,2,3]. These systems are usually based on centrifugal turbomechanisms, which are generally driven by squirrel cage induction motors (IMs).

The IMs possess high robustness, reliability and efficiency and they are relatively cheap [4]. Single-phase IMs are usually used only for low power applications where turbomechanisms' pressure or flow rate are regulated via valves/ducts. Three-phase IMs are used for a wide power range, and they can be combined with variable frequency drives (VFDs) to implement pressure or flow rate control according to consumers' demand. Since the power consumed by the turbomechanisms is proportional to their cubic velocity, there is a significant potential for energy savings during the transportation [5,6,7,8,9]. Interestingly, even simple pressure or flow rate stabilization systems allow to adjust automatically the turbomechanism's velocity depending on the air/water consumption to meet consumer demands. However, the implementation of such control requires installation of corresponding sensors. For low-power applications the cost of the pressure and flow rate sensors is comparable to the cost of the turbomechanisms, including their driving motors. That results in a new research direction in sensorless closed-loop control of the turbomechanisms, aiming to replace the expensive pressure and flow rate sensors by the estimators based on the IM's variables measurements, and to achieve the quality of control comparable to the systems utilizing pressure or flow rate sensors.

It is essential to acknowledge that the precision and dependability of these estimation techniques may be influenced by specific factors, notably the existence of solid particles within the water or air that the system circulates. In fact, as indicated in a study [10], estimating flow rate and pressure might prove to be unattainable in scenarios involving inhomogeneous water or air systems. This is attributed to the substantial fluctuation in power demands across various operational conditions, contingent on the quantity of solid particles in the system. Industrially produced sensorless controllers of centrifugal pumps are based on measurements of the IM's velocity and estimation of its input active power [11], usually available in the monitoring systems of VFDs. Further cost reduction of the turbomechanisms sensorless control implementation can be achieved via the motor's velocity estimation using only cheap current transducers for stator current measurements [12,13,14], which is quite popular and well-established area of research. The accuracy of the pressure and flow rate estimations can be improved via utilizing the estimated pump's shaft power instead of the estimated motor's input active power [11] since the estimation algorithms are based on the centrifugal pumps/fans pressure-flow rate and shaft power-flow rate curves determined experimentally at velocities. A simpler but less accurate solution is proposed in Ref. [15], where the reference frequency of the stator voltages is used instead of the velocity, combined with the input active power of the motor. It is based on the feed-forward backpropagation artificial neural networks (ANNs) trained based on the experimental data. The ANNs are also widely used in electric machines and power converters sensorless control [16,17,18,19].

Another popular estimation approach is based on the affinity laws of turbomechanisms. When the aerodynamic or hydraulic resistance of the network is constant, the flow rate is proportional to the velocity, and the pressure is proportional to the squared velocity. As a result, the estimations are very simple but have limited applicability [20].

The purpose of the present paper is to assess the further potential of applying ANNs for accurate prediction of the turbomechanisms' pressure and flow rate. Three inputs for the ANN estimators are considered, including the reference frequency of the stator voltages, the estimated active input power of the motor and the RMS value of the stator current. All three variables are typically accessed via monitoring systems in industrial VFDs, making it easy to embed the estimation algorithms into VFDs through software modification. Since the set of these inputs allows to determine the turbomechanisms'

velocity and shaft power, the accuracy of this new estimation algorithm improves compared to [15] and it is simpler compared to [12]. The proposed approach is verified using a specially developed test rig for rapid control prototyping of a centrifugal fan with induction motor drive based on dSpace DS1104 controller board. It provides more flexibility in research and design compared to using an industrial VFD. The control and estimation algorithms are designed in Matlab/Simulink environment and converted into the dSpace code. The “ControlDesk” software is used to create a virtual control panel to set the references and monitor the operation of the system.

The rest of the paper is structured as follows: First, a detailed description of the test rig and test procedure is provided. Following that, the paper presents the experimental data to be used in training ANNs and explains the design of the newly proposed pressure and flow rate ANN estimators. Consequently, the paper presents the verification of results and analyses the quality of the estimations.

2. EXPERIMENTAL TESTING OF A CENTRIFUGAL FAN FOR ESTIMATORS DESIGN

2.1. Test Rig Description

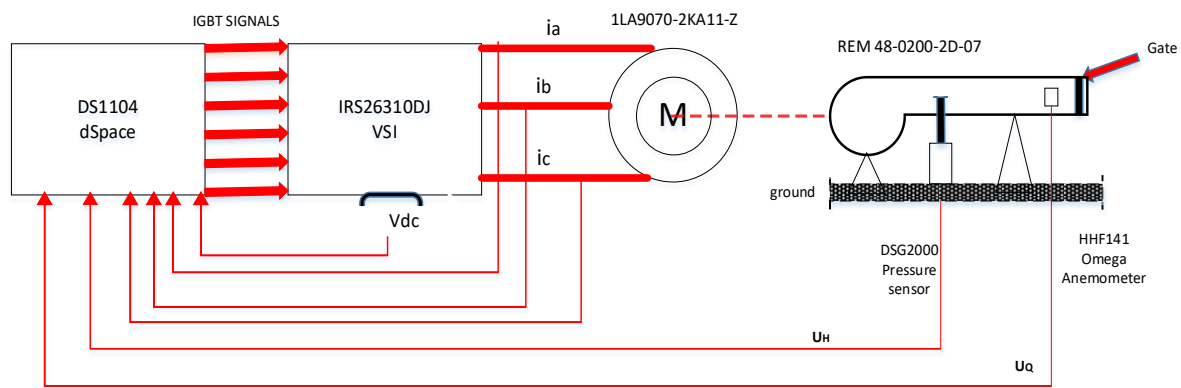


Figure 1. Functional block diagram of the control prototyping test rig of the centrifugal fan.

The industrial centrifugal fan REM 48-0200-2D-07 from Nicotra-Gebhardt is utilized in the test rig. The functional block diagram of the rig is depicted in Fig. 1. The optimal recommended operating point of the fan is with the flow rate of $1215 \text{ m}^3/\text{h}$ and the angular velocity of 2840 rpm. The static pressure achieved in this point is 680 Pa and the overall datasheet efficiency is 53.5%. The fan is equipped and driven directly by the Siemens three-phase squirrel cage induction motor 1LA9070-2KA11-Z. The rated power of the motor is 0.37 kW, and the rated velocity is 2840 rpm. The motor is delta connected and the rated voltage is 230 V. The parameters of the motor determined experimentally, using standard no-load and locked rotor tests are the stator resistance of 14.6 Ohm, the stator inductance of 1.1023 H, the rotor resistance of 16.53 Ohm, the rotor inductance of 1.1023 H, and the magnetizing inductance of 1.0541 H. The no-load test and locked rotor test require the motor dismounting from the fan since the fan always develops the motor load torque when moving and there is no mechanical way to lock the rotor. To avoid further complications with the motor remounting due to extremely high sensitivity to misalignment, an identical motor (without the fan) was bought from the fan manufacturer and tested.

The output of the fan is connected to an air duct as shown in Fig. 2. The output area of the duct is manually regulated from fully open to fully closed, using a gate. The air flow rate in the duct is measured by the Anemometer HHF141 Omega which turbine is mounted inside the duct. The air pressure in the duct is measured by the differential pressure sensor Ziehl Abegg DSG2000.

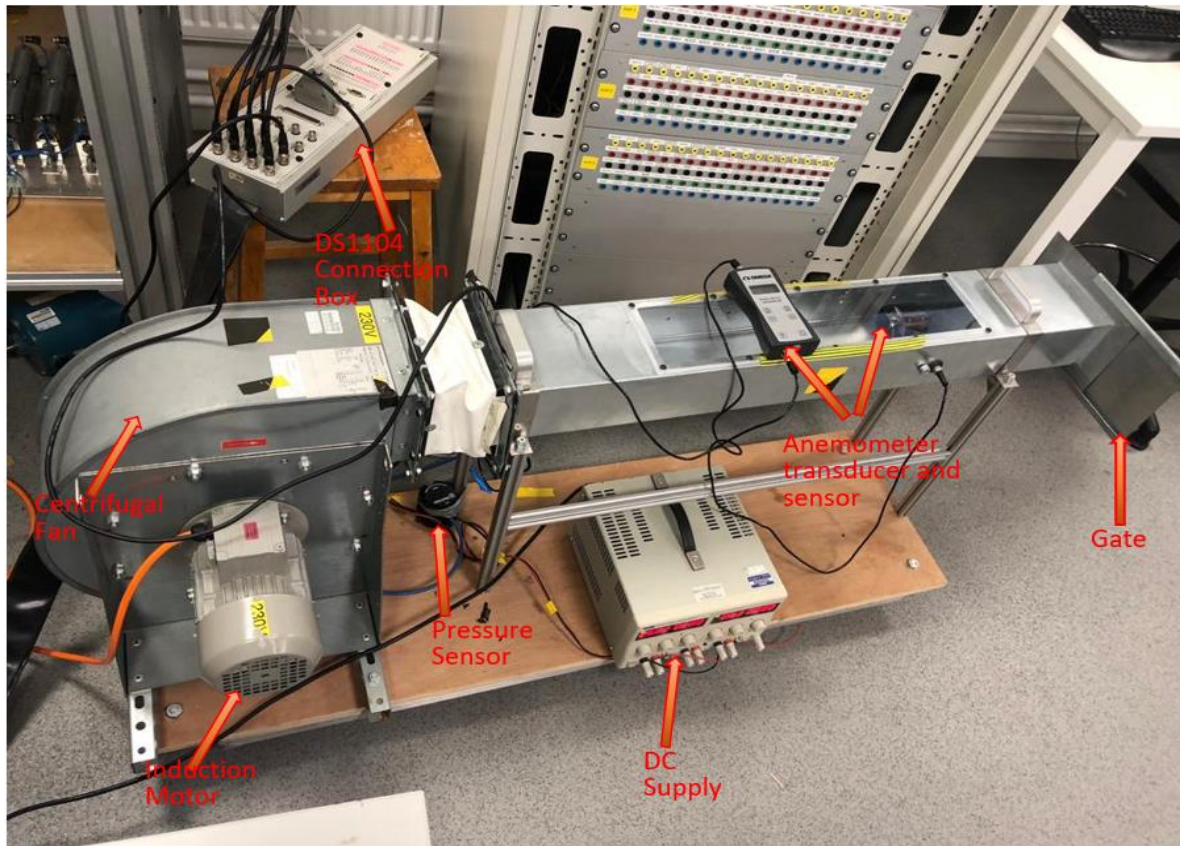


Figure 2. The test rig of the centrifugal fan.

The induction motor is supplied from the IRS26310DJ gate driver evaluation board, which implements a two-level full-bridge three-phase voltage source inverter (VSI) based on IGBTs fed from a single-phase full bridge diode rectifier through a DC link capacitor. The input rated voltage of the rectifier is 230 V_{RMS}. The continuous output rated power of the inverter is 400 W. The digital control of the evaluation board is switched off. The control pulses of the transistor switches are generated externally using dSpace DS1104 controller board connected to the VSI via digital isolators. The stator currents of the motor are measured using Hall effect-based transducers LTS 6-NP. The DC link voltage of the VSI is measured by the LV 25-P voltage transducer.

DS1104 implements the open loop control of the fan's velocity. It includes a ramp unit providing smooth increase of the motor voltage frequency reference, a functional block providing $V / f^2 = const$ control and a block generating the duty ratio three-phase references for the three-phase PWM generator imbedded into the DS1104 (see Fig. 3). The $V / f^2 = const$ control is a preferred option for centrifugal fans/pumps available in industrial VFDs along with the well-known $V / f = const$ control [21,22]. The centrifugal fans/pumps develop a 'fan' type of the load torque at the motor shaft; the load torque is proportional to the squared velocity. The critical torque of the induction motor under $V / f^2 = const$ control reduces with the frequency reduction (for $V / f = const$ it is almost constant) and its difference with the load torque at corresponding frequencies remains roughly the same allowing smooth transients even with the frequency step change. The experiments and design procedures presented in the paper can easily be replicated for $V / f = const$ control as well.

The sinusoidal PWM technique was selected for pulses generation. All sensors of the test rig are with analogue voltage outputs which are converted into digital through the ADC inputs of the DS1104.

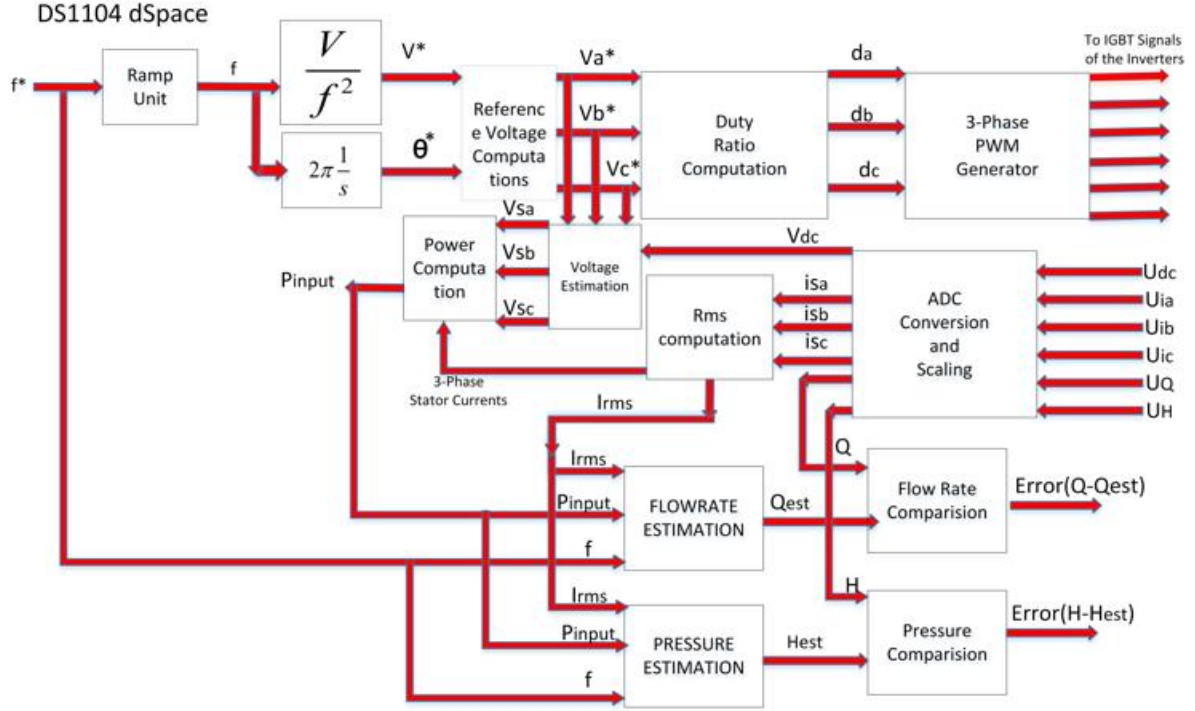


Figure 3. Block diagram of DS1104 based open-loop control of fan's velocity.

The RMS value of the stator line current is computed based on the instantaneous values of the stator line currents in each phase. In case the DC link voltage is constant, the fundamental components of the stator phase voltages are assumed to be equal to the corresponding reference voltages. Note that this is open loop scalar control without stator currents close loops. Therefore, there is no mechanism to adjust the voltage references due to PI currents controllers till the required currents are reached accurately. Additionally, due to the single-phase rectifier, the DC link voltage V_{dc} was found to be slightly floating. This means that the fundamental components of the stator voltages can also be floating. So the reference voltages V_a^* , V_b^* and V_c^* in Figure 3 are the initial voltage references scaled by the factor of $V_{dc\min} / V_{dc}$ to compensate the V_{dc} fluctuations, before being converted into the duty ratio references of the three legs of the VSI: d_a , d_b and d_c . As result, the instantaneous values of the fundamental components of the stator phase voltages are estimated based on the scaled stator reference voltages and the measured voltage of the DC link. The stator power is computed using the measured stator currents and the estimated voltages.

$$V_{sa} = \frac{1}{2} V_{dc} \frac{V_a^*}{V_m^*}, \quad V_{sb} = \frac{1}{2} V_{dc} \frac{V_b^*}{V_m^*}, \quad V_{sc} = \frac{1}{2} V_{dc} \frac{V_c^*}{V_m^*}, \quad (1)$$

$$V_{s\alpha} = V_{sa}, \quad V_{s\beta} = \frac{V_{sb} - V_{sc}}{\sqrt{3}}, \quad (2)$$

$$i_{s\alpha} = i_{sa}, \quad i_{s\beta} = \frac{i_{sb} - i_{sc}}{\sqrt{3}}, \quad (3)$$

$$P_{input} = \frac{3}{2} (i_{s\alpha} V_{s\alpha} + i_{s\beta} V_{s\beta}), \quad (4)$$

$$I_{rms} = \frac{\sqrt{\frac{2}{3} (i_{sa}^2 + i_{sb}^2 + i_{sc}^2)}}{\sqrt{2}}, \quad (5)$$

where i_{sa} , i_{sb} , i_{sc} and V_{sa} , V_{sb} , V_{sc} are the instantaneous values of the stator line currents and fundamental components of the phase voltages, respectively, $i_{s\alpha}$, $i_{s\beta}$ and $V_{s\alpha}$, $V_{s\beta}$ are the α and β components of the

stator current vector and stator fundamental voltage vector, respectively, in the stationary reference frame α - β . I_{rms} and P_{input} denote the stator RMS current and the stator active power. V_m^* is the maximum possible amplitude of the unscaled voltage references.

In Fig. 3, H , Q and H_{est} , Q_{est} are the measured pressure and flow rate and the estimated pressure and flow rate. U_{ia} , U_{ib} and U_{ic} are the output voltages of the current LTS 6-NP transducers, further converted into the stator currents values. U_{dc} is the output voltage of the LV 25-P voltage sensor, further converted into the DC link voltage value. Lastly, UQ and UH are the voltages proportional to the values of the flow rate and pressure measured by the Omega HHF141 Anemometer and the Ziehl Abegg DSG2000 differential pressure sensor, respectively.

2.2. Test Methodology for Data Acquisition

The width of the centrifugal fan's duct is 11 cm and it has been marked for each centimetre as shown in Figs. 4(a,b). The gate is used to close the duct of the system. If the position of the gate is at zero ($a=0$), this means the duct of the centrifugal fan is fully open. If the position of the gate is at $a=11$, the duct of the system is fully closed.

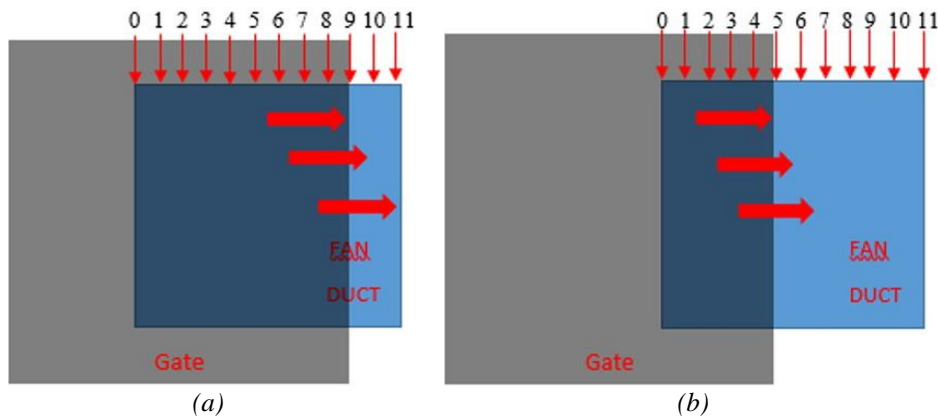


Figure 4. Fan obstruction at position (a) 9 cm and (b) 5 cm closed, respectively.

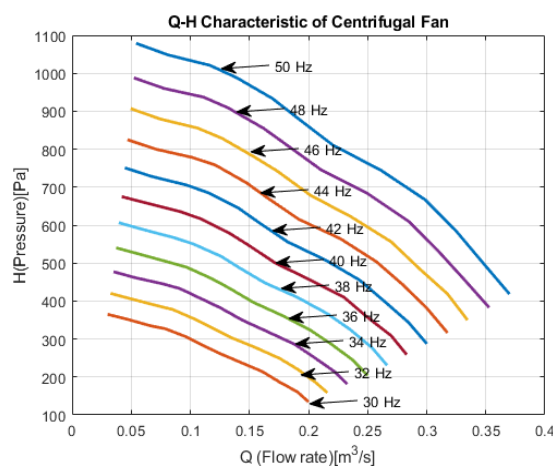


Figure 5. Q - H characteristics of the centrifugal fan.

To adjust the velocity of the system, the frequency is set constant at the intervals of 2 Hz between 30 Hz and 50 Hz. For each constant frequency, the gate position is changed between 0 and 11 with the step of 1 cm. Fig. 5 shows Q - H characteristics of the centrifugal fan obtained experimentally for 11 different frequencies. For each operating point corresponding to a specific frequency and gate position, the RMS

stator current value and the estimated input active power were recorded as well. In total, 132 operating points were tested.

3. ANN ESTIMATORS ARCHITECTURE AND TRAINING

The experimental data described in Section 2.1 are arranged into three arrays. The array of inputs contains information about the frequency, the RMS current and the input active power. The inputs array is depicted in Fig. 6 as a 3-D plot.

The first 11 columns of the inputs array are the values obtained for $a=0$ and for frequencies from 50 Hz to 30 Hz with the step 2 Hz. The final 11 columns are the values obtained for $a=11$ and the same frequencies. The arrangement is shown in Fig. 7. In particular, substantial differences in the lines between step changes result from the shift in frequency from 50 Hz to 30 Hz. The two target arrays contain the corresponding experimental pressure and flow rate values. This arrangement was found leading to more accurate estimation results comparing when the inputs array contains first information for 30 Hz, then for 32 Hz and etc, according to Fig. 5.

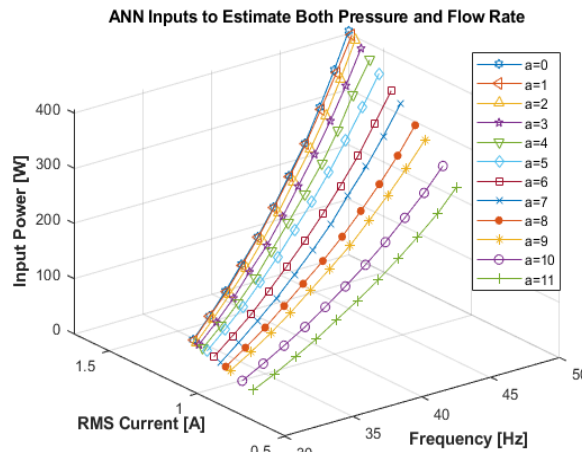


Figure 6. ANN inputs to estimate both pressure and flow rate.

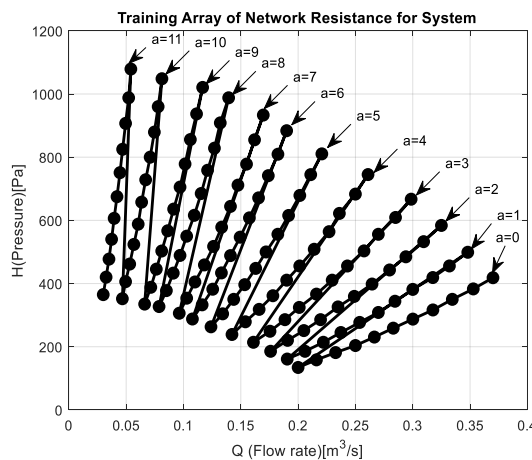


Figure 7. Training array of network resistance for system.

The feed-forward backpropagation ANN architecture is used to implement both pressure and flow rate estimators. For the flow rate estimation, a 3 layer ANN is used with 3, 3 and 1 neurons in each layer,

respectively. For the pressure estimation, a 3 layer ANN is used with 5, 5 and 1 neurons in each layer, respectively. Activation functions are chosen as hyperbolic tansig for the first and second layer neurons and as purelin for the output layer for both ANNs. The ANNs were created using MatLab nntool. The number of neurons in the first and second layers was determined iteratively as minimum possible and providing the estimation accuracy satisfying the ISO 13348 standard.

Bayesian Regularization (trainbr in Matlab) is used, for both flow rate and pressure estimations, as a training function owing to the fact that it can provide good generalization for the systems which have difficult, small and noisy datasets. The gensim Matlab command converts the trained ANNs into Simulink blocks which are added into the Simulink model for DS1104 implementing the algorithm of Fig. 3, allowing to compare the measured and estimated values of the pressure and flow rate. The sampling time of the ANNs and the whole control algorithm are the same as 0.01 s.

4. RESULTS AND DISCUSSION

The ISO 13348 standard requires +/-5% pressure accuracy, +/-5% flow rate accuracy and +/-8% power accuracy. This section assesses the accuracy of the pressure and flow rate estimators with different set of the inputs. The number of layers and neurons remain the same. The same activation functions are used. However, the ANNs are trained accordingly based on the modified input arrays.

Fig. 8 and Fig. 9 show the error of steady state pressure estimation with respect to the experimental data for 4 cases of the inputs set, for the trained 132 operating points. Similar results are depicted in Fig. 10 and Fig. 11 for steady state flow rate estimation with respect to the corresponding experimental data. The smallest discrepancy between the experimental and estimated data is when the inputs are frequency, RMS stator current and consumed active power. In this case the error of the pressure estimation is between -3.8% and +4%, and for the flow rate it is between -4.1% and +4.2%. The best results compared to the estimators with the different inputs, including the simplest and tested in [13] with the frequency and the input active power only as inputs, are because this set of parameters contains the most accurate information of the motor velocity and fan's shaft power. Interestingly, that even the set including the input active power and the RMS stator current is sufficient for the pressure and flow rate estimation.

Both the pressure sensor and flow rate sensor brands shown in Fig. 1 have a measurement accuracy of ± 0.25 . This implies that the overall impact on the difference between experimental pressure and flow rate measurement and pressure and flow rate estimated data are significant. After accounting for the accuracy of the sensors, the error percentage of the pressure estimation is expected to be within the range of -4.05% to +4.25%. Similarly, for the flow rate, the error is anticipated to be between -4.35% and +4.45%. However, these values remain within the acceptable limits defined by the ISO standard.

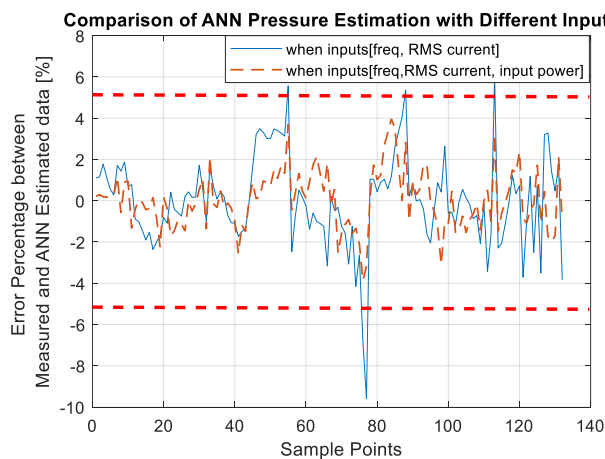


Figure 8. Comparison of ANN pressure estimation with different inputs.

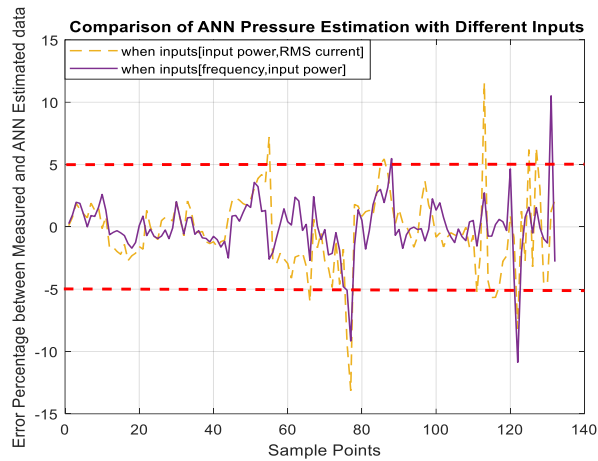


Figure 9. Comparison of ANN pressure estimation with different inputs.

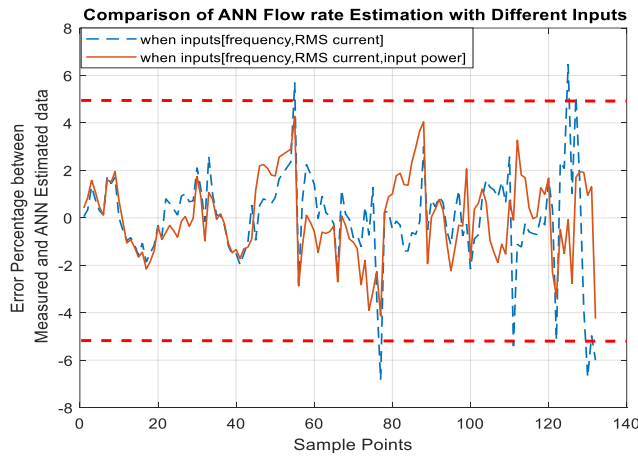


Figure 10. Comparison of ANN flow rate estimation with different inputs.

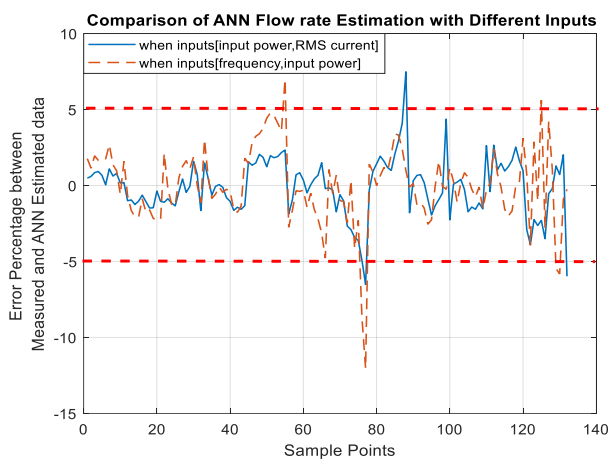


Figure 11. Comparison of ANN flow rate estimation with different inputs.

Fig. 12, Fig. 13, Fig. 14 and Fig. 15 demonstrate the accuracy of the estimation of the flow rate and pressure with respect to the experimental data presented for all positions of the fan’s gate, for the algorithm with the three input signals. The smallest discrepancy for the flow rate and pressure estimations are in position 3 (+1.7467% - 0.9748%) and position 4 (-0.4189% + 0.1013%), respectively.

The worst flow rate estimation is for position 11, where the fan's gate is completely closed, and the flow rate is the smallest measured. The worst pressure estimations are for positions 0 and 1 where the fan's gate is fully opened, and the measured pressure is the lowest measured. This is as expected since the relative error is higher for the lower measured values. Note that these positions are boundary for the duct and the fan is usually selected to work mainly in the middle positions.

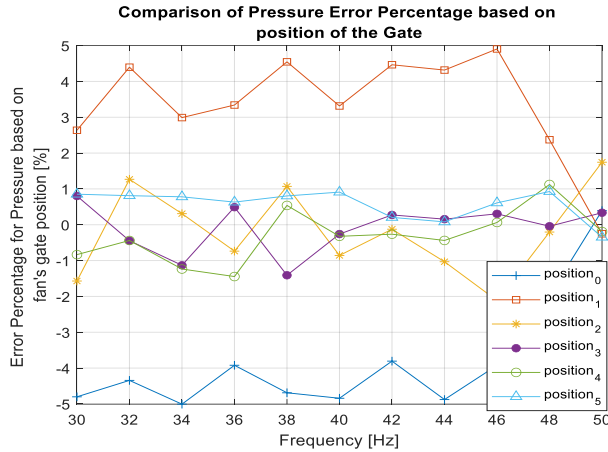


Figure 12. Comparison of pressure error percentage based on position of the gate.

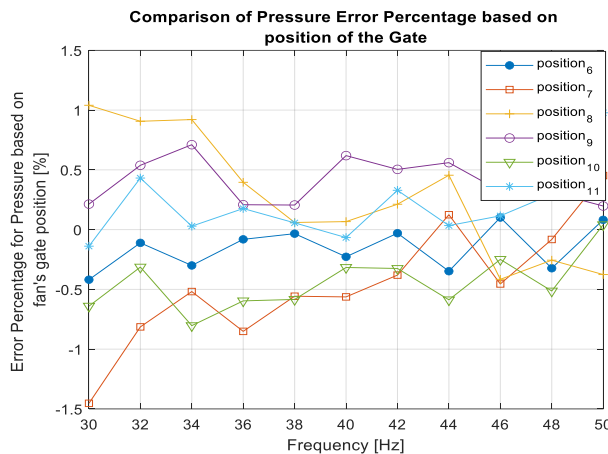


Figure 13. Comparison of pressure error percentage based on position of the gate.

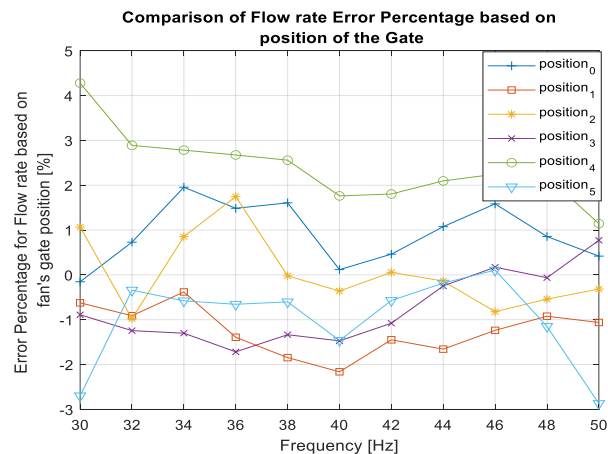


Figure 14. Comparison of flow rate error percentage based on position of the gate.

The ANN pressure and flow rate estimators were imbedded into the test rig control algorithm and verified experimentally for the operating points not used for ANNs training, gate position 7 and odd values of the frequency between 31 Hz and 49 Hz. As can be seen from Fig. 16, the error percentage between experimental and estimated data is also within the range of the ISO standard.

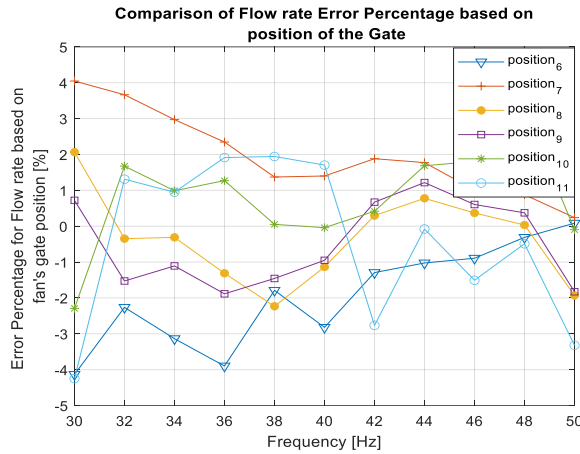


Figure 15. Comparison of flow rate error percentage based on position of the gate.

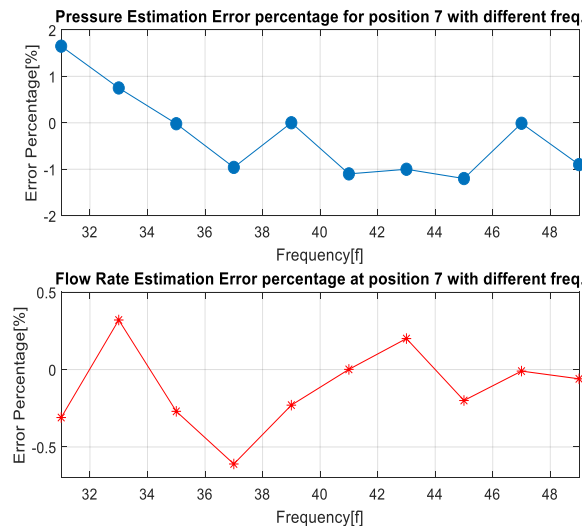


Figure 16. Pressure estimation error percentage for position 7 with different frequencies.

The comparison of the obtained results with other methods are shown in Table 1. The accuracy of the estimations is improved both for pressure and flow rate estimations compared to the existing approach without the measured RMS stator current. When the existing approach is employed, which relies on velocity (or frequency) and input power, the estimation results in an error rate of more than 11% for pressure and over 12% for flow rate. However, with a new and simplified estimation method, the maximum error percentages are reduced to 4% for pressure and 4.2% for flow rate, respectively. It does not make the estimations more complicated since all three inputs of the estimators are accessible through the monitoring systems of industrial VFDs and are either extracted from control algorithm or based on relatively cheap current transducers.

In addition, the paper [23] develops a universal model of a centrifugal pump operating as a turbine. The parameters of the model are determined based on the data sheet without knowledge of the pump geometry. Nevertheless, the model's complexity, characterized by an excessive number of parameters, renders it challenging for control design and simulation purposes. Notably, when employed without

knowledge of the pump's geometry, it exhibits an error rate of approximately 21.4% at optimal operating conditions, which reduces to 7.2% when geometric information is accounted for. Furthermore, the study discussed in reference [24] examines the estimation of head and flow rate in a scenario where the motor is supplied by a constant AC voltage source, such as an AC grid. It illustrates the implementation of motor velocity and shaft power estimation techniques, facilitating subsequent estimation of head and flow rate through a QP curve-based methodology. Reported findings indicate a 16% error in flow rate estimation and a 3.2% error in shaft power prediction utilizing this approach. While the method's simplicity is noted, its accuracy for sensorless control is limited, albeit falling within acceptable ranges for pressure estimation. Nevertheless, it holds potential for application in energy audit procedures for high-power pump systems.

Table 1. Comparison of obtained results with the literature.

Number	Method	Max. Discrepancy of Flow Rate Estimation [%]	Max. Discrepancy of Pressure Estimation [%]
1	Obtained Novel Method	4.45%	4.25%
2	ANN (Freq. and Input Power)	12.5%	13%
3	ANN (RMS Current and Input Power)	7.7%	15%
4	ANN (Freq. and RMS Current)	8.05%	9.6%
5	Model Estimating of a Centrifugal Pump operating as a Turbine [23]	7.2%	7.2%
6	Q-P Curve-based Estimation [24]	%16	within the range of +/-5%

5. CONCLUSION

The paper has made substantial contributions to the domain of state estimation and control in centrifugal fans and pumps with induction motor drives. It introduces a novel approach for the estimation of pressure and flow rate in these systems, which relies on feed-forward backpropagation neural networks. This novel approach necessitates input data, specifically the stator voltages frequency, the estimated motor in. The proposed method achieves a maximum error of only 4% for pressure and 4.2% for flow rate, demonstrating its effectiveness. put active power, and the measured RMS stator current. The investigation also confirms that the estimations are feasible, although less accurate, if only the frequency and the RMS stator current, or the RMS stator current and the input motor active power are used as the two inputs for the estimators. The paper also presents a test rig for the fan's control prototyping, which allows accurate data collection for the necessary ANNs training and reveals features that useful for practical engineers regarding the design and testing procedure.

REFERENCES

- [1] de Almeida, AT, Fonseca, P, Falkner, H, Bertoldi, P. Market transformation of energy-efficient motor technologies in the EU. *Energy Policy* 2003; 31: 563-575. DOI: 10.1016/S0301-4215(02)00100-3
- [2] Abdelaziz, EA, Saidur, R, Mekhilef, S. A review on energy saving strategies in industrial sector. *Renewable and Sustainable Energy Reviews* 2011; 15: 150-168. DOI: 10.1016/j.rser.2010.09.003
- [3] Waide, P, Brunner, CU. Energy-efficiency policy opportunities for electric motor-driven systems. *International Energy Agency* 2011; na: 132. DOI: 10.1787/5kkg52gb9gjd-en
- [4] Almounajjed, A, Sahoo, AK, Kumar, MK, Assaf, T. Fault diagnosis and investigation techniques for induction motor. *International Journal of Ambient Energy* 2022; 43: 6341-6361. DOI: 10.1080/01430750.2021.2016483
- [5] Binder A. Potentials for energy saving with modern drive technology-a survey. In: SPEEDAM 2008 Proceedings of 19th International Symposium on Power Electronics, Electrical Drives, Automation and Motion, June 2008: Ischio, Italy: pp. 90-95.
- [6] Ferreira, FJTE, Fong, JAC, de Almeida, AT. Ecoanalysis of variable-speed drives for flow regulation in pumping systems. *IEEE Transactions on Industrial Electronics* 2011; 58: 2117-2125. DOI: 10.1109/TIE.2010.2057232

- [7] Kiselychnyk, O, Bodson, M, Werner, H. Interactive energy saving control of water supply pump based on pressure measurement. *Transactions of Kremenchuk State Polytechnic University* 2009; 56: 166-171 <<https://ela.kpi.ua/handle/123456789/38238>>
- [8] Kiselychnyk O, Bodson M, Werner H. Overview of energy efficient control solutions for water supply systems. In: KSPU 2009 Transactions of Kremenchuk State Polytechnic University 2009; Kremenchuk, Ukraine: pp. 40–45.
- [9] de Almeida, AT, Ferreira, FJTE, Both, D. Technical and economical considerations in the application of variable-speed drives with electric motor systems. *IEEE Transactions on Industry Applications* 2005; 41: 188-199. DOI: 10.1109/TIA.2004.841022
- [10] Making Sense of Sensorless - Empowering Pumps and Equipment.pdf [Internet]. [cited 2023 Oct. 23]. Available from: <https://empoweringpumps.com/making-sense-sensorless>.
- [11] Kiselychnyk, O, Bodson, M. Nonsensor control of centrifugal water pump with asynchronous electric-drive motor based on extended Kalman filter. *Russian Electrical Engineering* 2011; 82: 69-75. DOI: 10.3103/S1068371211020088
- [12] Wu, Q, Shen, Q, Wang, X, Yang, Y. Estimation of centrifugal pump operational state with dual neural network architecture-based model. *Neurocomputing* 2016; 216: 102–108. DOI: 10.1016/j.neucom.2016.07.035
- [13] Ahonen, T, Tamminen, J, Ahola, J, Viholainen, J, Aranto, N, Kestilä, J. Estimation of pump operational state with model-based methods. *Energy Conversion and Management* 2010; 51: 1319-1325. DOI: 10.1016/j.enconman.2010.01.009
- [14] Tamminen J, Ahonen T, Ahola J, Kestilä J. Sensorless flow rate estimation in frequency-converter-driven fans. In: EPE 2011 Proceedings of the 2011-14th European Conference on Power Electronics and Applications: Birmingham, United Kingdom: pp. 1-10.
- [15] Pechenik, M, Kiselychnyk, O, Buryan, S, Petukhova, D. Sensorless control of water supply pump based on neural network estimation. *Electrotechnic and Computer Systems* 2011; 3: 462-466 <<https://eltechs.op.edu.ua/index.php/journal/article/view/790>>
- [16] Bose, BK. Expert system, fuzzy logic, and neural network applications in power electronics and motion control. In *Proceedings of the IEEE* 1994; 82: 1303-1323. DOI: 10.1109/5.301690
- [17] Lee, HY, Lee, JL, Kwon, SO, Lee, SW. Performance estimation of induction motor using artificial neural network. In: IWSSIP 2018 25th International Conference on Systems, Signals and Image Processing 2018; Ohrid, North Macedonia: pp. 1-3.
- [18] Ebrahim, OS, Badr, MA, Elgendy, AS, Jain, PK. ANN-based optimal energy control of induction motor drive in pumping applications. *IEEE Transactions on Energy Conversion* 2010; 25: 652-660. DOI: 10.1109/TEC.2010.2041352
- [19] Wlas, M, Krzeminski, A, Guzinski, J, Abu-Rub, H, Toliyat, HA. Artificial-neural-network-based sensorless nonlinear control of induction motors. *IEEE Transactions on Energy Conversion* 2005; 20: 520-528. DOI: 10.1109/TEC.2005.847984
- [20] Tamminen, J, Viholainen, J, Ahonen, T, Ahola, J, Hammo, S, Vakkilainen, E. Comparison of model-based flow rate estimation methods in frequency-converter-driven pumps and fans. *Energy Efficiency* 2014; 7: 493–505. DOI: 10.1007/s12053-013-9234-6
- [21] Altivar Machine ATV320 Variable Speed Drives for Asynchronous and Synchronous Motors Installation Manual.pdf [Internet]. [cited 2023 Oct. 22]. Available from: <https://download.schneider-electric.com>.
- [22] ACS550 User's Manual ACS550-01 Drives (0.75...160 kW) ACS550-U1 Drives (1...200 hp).pdf [Internet]. [cited 2023 Oct 22]. Available from: <https://library.e.abb.com>.
- [23] Barbarelli, S, Amelio, M, Florio, G. Predictive model estimating the performances of centrifugal pumps used as turbines. *Energy* Jul. 2016; 107: 103–121. DOI: 10.1016/J.energy.2016.03.122.
- [24] Ahonen, T, Kortelainen, JT, Tamminen, JK, Ahola, J. Centrifugal pump operation monitoring with motor phase current measurement. *International Journal of Electrical Power Energy Systems* 2012; 42: 188-195. DOI: 10.1016/j.ijepes.2012.04.013.